The Electronic Structure and Vibrational Spectrum of *trans*-HNOO†

Roger L. DeKock,*,‡,⊗ Michael J. McGuire,§ Piotr Piecuch,*,§,@ Wesley D. Allen,*,||,+ Henry F. Schaefer, III,|| Karol Kowalski,§ Stanisław A. Kucharski,⊥ Monika Musiał,⊥ Adam R. Bonner,‡ Steven A. Spronk,‡ Daniel B. Lawson,# and Sandra L. Laursen$^{\nabla}$

Department of Chemistry and Biochemistry, Calvin College, Grand Rapids, Michigan 49546, Department of Chemistry, Michigan State University, East Lansing, Michigan 48824, Center for Computational Chemistry, University of Georgia, Athens, Georgia 30602, Institute of Chemistry, University of Silesia, Szkolna 9, 40-006 Katowice, Poland, Department of Natural Sciences, University of Michigan-Dearborn, Dearborn, Michigan 48128, and Cooperative Institute for Research in Environmental Sciences, University of Colorado, Boulder, Colorado 80309

Received: September 19, 2003; In Final Form: December 18, 2003

This paper reports the theoretical results of a thorough, state-of-the-art, coupled-cluster, renormalized coupled-cluster, and vibrational study on the molecule imine peroxide, HNOO, in its trans conformation. This molecule is isoelectronic with ozone and presents many of the same difficulties for theory as ozone. We report both the theoretical geometry and the vibrational frequencies, including anharmonic corrections to the computed harmonic vibrational frequencies obtained by calculating the quartic force field at the high levels of coupled cluster theory, including CCSD(T) and its renormalized and completely renormalized extensions and methods including the combined effect of triply and quadruply excited clusters [CCSD(TQ_f) and CCSDT-3(Q_f)]. The motivation behind our study was the disagreement between two previous reports that appeared in the literature on HNOO, both reporting theoretical (harmonic) and experimental (matrix isolation) vibrational spectra of HNOO. Our new theoretical results and our analysis of the previous two papers strongly suggest that the correct assignment of vibrational spectra is that of Laursen, Grace, DeKock, and Spronk (*J. Am. Chem. Soc.* **1998**, *120,* 12583−12594). We also compare the electronic structure of HNOO with the isoelectronic molecules HONO and O_3. The NO and OO bond lengths are practically identical in HNOO, in agreement with the identical OO bond lengths (by symmetry) in ozone. Correspondingly, the NO and OO stretching frequencies of *trans*-HNOO are in close proximity to each other, as are the symmetric and antisymmetric OO stretching frequencies in O_3. This is in contrast to the electronic structure of HONO, which has a large difference between the two NO bond lengths, and a correspondingly large difference between the two NO vibrational frequencies. These results are readily understood in terms of simple Lewis electron dot structures.

Introduction

The new molecule imine peroxide, HNOO, appeared in the title of two papers in back-to-back issues of the *Journal of the American Chemical Society* in December, 1998. The first, by Ling, Boldyrev, Simons, and Wight (LBSW),[1] was entitled "Laser Photolysis of Matrix-Isolated Methyl Nitrate: Experimental and Theoretical Characterization of the Infrared Spectrum of Imine Peroxide (HNOO)". The second, by Laursen, Grace, DeKock, and Spronk (LGDS),[2] was entitled "Reaction of NH (X) with Oxygen in a Solid Xenon Matrix: Formation and Infrared Spectrum of Imine Peroxide, HNOO". Both of these papers relied on the same general experimental techniques (photolysis, matrix isolation, and infrared spectroscopy) and similar electronic structure methods (ab initio and density functional theory). Examination of the reported infrared spectra shows that the two papers obviously are reporting on different molecules. The differences in the infrared spectra assigned to HNOO are large, see Table 1. The assignment of the frequencies according to the type of motion was done only by LGDS. These assignments of vibrational motion are obviously only approximate, except for the torsional motion which is separated by symmetry from the remainder of the motions. This approximate assignment of motions will be useful in our discussion throughout this paper.

The work of LBSW was done in argon matrices and that of LGDS in xenon matrices, but this difference is not sufficient to account for the wide frequency disparities.[3] Some work using Ar matrices is reported by LGDS, and the differences between Xe and Ar matrices are small. Furthermore, the reported relative intensities do not agree for the different bands. A crucial factor in comparing these two sets of results is the assignment made to ν_3 and ν_4, corresponding to the NO and OO stretching motions. LBSW assign these at 1381.6 and 843.2 cm^{-1}, whereas LGDS assign them at 1092.3 and 1054.5 cm^{-1}. For the former, this is a $\nu_3 - \nu_4$ difference of ~550 cm^{-1}, whereas for the latter it is ~50 cm^{-1}. According to Badger's rule,[4−6] these results, in

† Part of the special issue "Fritz Schaefer Festschrift".

* Corresponding authors.
‡ Calvin College
§ Michigan State University.
|| University of Georgia.
⊥ University of Silesia.
University of Michigan-Dearborn.
$^{\nabla}$ University of Colorado.
⊗ E-mail: dekock@calvin.edu.
@ E-mail: piecuch@cem.msu.edu.
+ E-mail: wdallen@ccqc.uga.edu.

10.1021/jp036809q CCC: $27.50
Published on Web 02/12/2004

TABLE 1: Experimental Results for HNOO Reported by LBSW and LGDS[a]

frequency	LBSW (ref 1)	LGDS (ref 2)
ν_1 (NH str)	3287.7 (3.12)	3165.5 (0.07)
ν_2 (HNO bend)	not obs.	1485.5 (0.12)
ν_3 (NO str)	1381.6 (0.74)	1092.3 (1.00)
ν_4 (OO str)	843.2 (0.35)	1054.5 (0.25)
ν_5 (NOO bend)	670.1 (0.19)	not obs.
ν_6 (torsion)	790.7 (0.32)	764.0 (0.57)

[a] Frequencies in cm^{-1}, relative intensities in parentheses. See refs 1 and 2 for details regarding the relative intensities.

turn, imply that there is a large difference between the NO and OO bond lengths for the molecule assigned by LBSW, whereas there is a small difference between these two bond lengths for the molecule reported by LGDS. If HNOO has a large difference in the NO and OO bond lengths it will behave like HONO, whereas if there is a small difference between these two bond lengths it will behave similarly to ozone.

There are at least three reasons why the above discrepancies between the results of the LBSW and LGDS studies deserve a thorough theoretical examination. First, there is an obvious need to determine which (if any) of the two interpretations of the observed vibrational spectra is correct. The discrepancies between the LBSW and LGDS data are so large that only one of these two groups can have spectroscopic evidence for the existence of HNOO. In such a situation, a thorough theoretical study employing state-of-the-art computational methods based on first principles of quantum mechanics is essential. The purported HNOO molecule contains only four atoms. For such a "small" molecule, a thorough ab initio computational work should be able to predict the vibrational frequencies with very high accuracy, allowing one to distinguish between the disparate assignments in the reported infrared spectra. In particular, the HNOO molecule is small enough to allow for a large number of high-level ab initio calculations based on the coupled cluster theory[7,8] (cf. refs 9−12 for selected reviews) and its renormalized and completely renormalized extensions.[12−15] The ability of the standard coupled-cluster method with singles, doubles, and noniterative triples [CCSD(T)][16] and its higher-order extensions accounting for the effects of singly, doubly, triply, and quadruply excited clusters, such as CCSD(TQ_f),[17] to accurately describe geometries, vibrational frequencies, and other properties of molecular systems is well known.[9−11,14,15] The renormalized and completely renormalized coupled cluster approaches of Kowalski and Piecuch[12−15] provide further improvements in the results of the CCSD(T), CCSD(TQ_f), and similar calculations when the nondynamical correlation effects become important.[12−15,18−26]

Second, HNOO is isoelectronic with both HONO and O_3. Both of these molecules are implicated in atmospheric chemistry[27] and are therefore of interest to the chemistry community. Since the electronic structures of HONO and O_3 are quite different, we want to determine whether HNOO mimics one of these or the other, or if it is unique.

Third, the isoelectronic molecule O_3 has been the subject of numerous theoretical studies for two reasons: (1) its multireference character[28,29] and significance of higher-order correlation effetcts,[30,31] and (2) its importance in environmental chemistry. Although CCSD(T), CCSD(TQ_f), and similar coupled cluster methods are formally single-reference methods, they can very accurately describe high-order correlation effects, even in situations characterized by significant multireference character of the many-electron wave function. In particular, the CCSD(T) and CCSD(TQ_f) methods are known to provide a very good description of the harmonic vibrational frequencies of ozone,[30−32] successfully competing with multireference methods. It is, therefore, very likely that these and related coupled cluster methods will provide us with a definitive, high-quality description of the HNOO vibrational spectrum. We might add that the multireference character of HNOO is a consequence of its expected diradical nature, commented upon before.[33] For systems having multireference and/or diradical character, the renormalized and completely renormalized CCSD(T) methods[12−15] perform remarkably well, improving the results of the standard CCSD(T) calculations[26] (cf., also, refs 12−15, 19−21, and 23−25). It is, therefore, very interesting to examine how reliable the renormalized and completely renormalized CCSD(T) approaches are in the case of HNOO.

Two close-lying geometric isomers are possible for HNOO, cis and trans. Both LBSW and LGDS present evidence for only one isomer in the matrix. Although it is not certain in either work which of the two forms was experimentally observed, both papers state that the agreement between theory and experiment is better for the trans isomer. Hence, this paper focuses only on theoretical work for the trans isomer. We have completed some preliminary theoretical work on the cis isomer, but this information does not alter our analysis of the trans species. The detailed ab initio study of the cis species will be discussed in a separate paper. Further details related to a comparison of the cis and trans isomers are presented in the Appendix.

It is the purpose of this paper to report thorough coupled cluster studies on *trans*-HNOO: geometry, harmonic vibrational frequencies, and, above all, anharmonic corrections to the frequencies. We then compare the calculated vibrational frequencies with the experimental results of LBSW and LGDS, and conclude that only the LGDS report is the correct assignment of the spectral lines for HNOO. The calculation of anharmonic corrections to vibrational frequencies is accomplished by generating several highly accurate quartic force fields for *trans*-HNOO that correspond to different coupled cluster approaches employed in this work, using the theoretical methodology developed in refs 34−38. The reliable information about the quartic force field and frequencies of fundamental vibrational transitions corrected for anharmonicities, obtained in this work, is of primary importance for our discussion, since one of the main goals of the present study is to answer a basic question, which of the two assignments of vibrational spectra reported by LBSW and LGDS is correct. By having access to "true" frequencies of fundamental vibrational transitions of the *trans*-HNOO isomer, resulting from a careful anharmonic analysis of the highly accurate ab initio electronic structure data, we eliminate the risk of misinterpreting the spectrum by comparing the frequencies of the fundamental vibrational transitions observed in experiment with the approximate vibrational frequencies resulting from harmonic analysis. As part of our discussion, we critique both the theoretical and experimental results of both LBSW and LGDS. Furthermore, we compare our results for HNOO to those of the isoelectronic molecules HONO and O_3. We conclude that the electronic structure of HNOO is similar to that of O_3, and unlike that of HONO.

This paper is organized as follows. (1) We introduce the computational methods that have been employed, including the treatment of the electronic structure problem and methods used to generate the quartic force field of *trans*-HNOO. (2) We present our results for several ab initio methods, focusing on the aforementioned high-level coupled-cluster methods and their renormalized and completely renormalized variants. (3) We compare these new theoretical results with the experimental

results of LBSW and LGDS.(4) We critique the experimental and theoretical work of both LBSW and LGDS. (5) We compare our work on HNOO to other experimental and theoretical work on HONO and O_3, to place the HNOO molecule in context. (6) We summarize our findings.

Computational Methods

Our calculations were performed in two steps. First, we carried out the electronic structure calculations of the optimum geometry and ground-state potential energy surface of *trans*-HNOO required to generate the quartic force field for the subsequent vibrational analysis, using a variety of coupled cluster methods. Next, the information about the ground-state potential energy surface of *trans*-HNOO was used to determine the harmonic and anharmonic force constants, from which we determined the final vibrational frequencies. We begin our description of the computational procedures employed in this study with the discussion of the electronic structure calculations.

The electronic structure calculations were initiated by optimizing the geometry of *trans*-HNOO using the coupled cluster CCSD(T) approach[16] and the cc-pVTZ basis set.[39] Because of the need for high precision in the calculations of quartic force fields, we used very tight convergence criteria for the restricted Hartree−Fock (RHF) and CCSD (coupled cluster singles and doubles) calculations that preceded the determination of the CCSD(T) energies and gradients. Thus, we converged the RHF equations to 10^{-12} for the maximum change in the SCF density matrix and the CCSD equations to 10^{-12} for the maximum change in cluster amplitudes defining the CCSD wave function. In addition, we kept all transformed integrals in the calculations by setting the relevant cutoff thresholds at 10^{-20} hartree or less. The CCSD(T) geometry optimization was carried out until the calculated RMS energy gradient was smaller than 10^{-10} hartree/bohr. To facilitate the geometry optimization and maintain high numerical precision throughout the calculations, we used the analytic gradient capability offered for the CCSD(T) approach by ACES II.[40] As in the case of the CCSD amplitude equations, the CCSD so-called Λ equations,[41,42] which have to be solved to calculate the CCSD(T) energy gradient, were converged to 10^{-12} for the maximum change in the coefficients defining the relevant CCSD Λ vector.

Once the equilibrium geometry of *trans*-HNOO was determined with the analytic CCSD(T) gradients, we generated a common grid of 263 nuclear geometries, centered on the CCSD(T) optimum geometry as the reference structure, required for the subsequent anharmonic vibrational analysis. We used this grid to perform additional electronic structure calculations, using a variety of coupled cluster methods, to obtain a few different force fields for the *trans*-HNOO molecule. Further details related to the grid generation procedure and subsequent anharmonic vibrational analysis are described in a later part of this section. The coupled cluster methods used to perform the electronic structure calculations are discussed first.

The basic force field for the present study of the vibrational spectrum of *trans*-HNOO was obtained by performing the CCSD(T) calculations, using the grid of 263 nuclear geometries mentioned above. We used the same cc-pVTZ basis set and the same, very tight, convergence criteria for solving the coupled cluster equations at each nuclear geometry from the grid as used during the CCSD(T) geometry optimization. To test the reliability of the resulting CCSD(T) vibrational frequencies, we performed several additional calculations with state-of-the-art coupled-cluster methods [CCSD(TQ_f) and CCSDT-3(Q_f)[17]] that account for the high-order many-electron correlation effects due to connected quadruply excited clusters neglected in the CCSD(T) calculations, and with the renormalized and completely renormalized CCSD(T) approaches [R−CCSD(T) and CR−CCSD(T), respectively][12−15] that may provide further improvements in the description of diradical molecular systems, such as HNOO.

The need for the additional CCSD(TQ_f) and CCSDT-3(Q_f) calculations is justified by the fact that the HNOO molecule is isoelectronic with ozone. It has been established that a highly accurate description of the harmonic frequencies of ozone (errors on the order of 10 cm^{-1}) requires the explicit inclusion of the connected quadruply excited clusters in the calculations.[17,30,31] The CCSD(TQ_f) and CCSDT-3(Q_f) methods allow us to examine the effect of quadruply excited clusters without having to deal with the prohibitive costs of the full CCSDTQ (coupled cluster singles, doubles, triples, and quadruples)[43−46] calculations. Recall that the CCSD(TQ_f) method represents an extension of the standard CCSD(T) approach in which, in addition to the noniterative energy corrections to the CCSD energy due to triply excited clusters that are already present in the CCSD(T) theory, one considers the noniterative energy corrections due to quadruply excited clusters.[17] The main advantage of the CCSD(TQ_f) approximation is the relatively low cost of calculating the corrections due to quadruples. The most expensive steps in the calculation of the noniterative quadruples (Q_f) corrections scale as $n_o^2 n_u^5$, where n_o and n_u are the numbers of occupied and unoccupied orbitals, respectively. This should be compared with the usual and manageable noniterative $n_o^3 n_u^4$ steps of the CCSD(T) theory, and the prohibitively expensive $n_o^4 n_u^6$ steps of the CCSDTQ approach, which accounts for the quadruply excited clusters in the fully iterative fashion.[43−46] As one can see, the cost of calculating the noniterative (Q_f) correction is not much greater than the cost of calculating the standard triples (T) correction of CCSD(T). To verify if the noniterative treatment of triples in the CCSD(T) and CCSD(TQ_f) approaches is sufficient to obtain the desired accuracies, we also performed the CCSDT-3(Q_f) calculations. The CCSDT-3(Q_f) approach represents an extension of the CCSD(TQ_f) method, in which one adds the same type of the noniterative energy correction due to quadruply excited clusters as used in the CCSD(TQ_f) approach to the CCSDT-3 energy.[47] Unlike CCSD(T), the CCSDT-3 approach, on which the CCSDT-3(Q_f) method is based, is an iterative triples method. For all practical purposes, the CCSDT-3 approach provides results of full CCSDT (coupled cluster singles, doubles, and triples) quality,[48,49] but computer costs of the CCSDT-3 calculations are smaller than costs of the full CCSDT calculations.[47] Thus, the CCSDT-3(Q_f) method can be viewed as an approach which provides results of very high CCSDT(Q_f) quality[17] (highly accurate results in which noniterative corrections due to quadruples are added to the full CCSDT energies) at a fraction of the computer cost associated with the CCSDT(Q_f) calculations.

The CCSD(TQ_f) calculations were performed on the same grid of 263 nuclear geometries as used in the CCSD(T) calculations. Unfortunately, we were unable to do the same for the CCSDT-3(Q_f) method. Although the CCSDT-3(Q_f) method is less expensive than the CCSDT(Q_f) and CCSDTQ approaches, the computer costs of the CCSDT-3(Q_f) calculations for the cc-pVTZ HNOO molecule make it very difficult to obtain all 263 energy values in a reasonable time (despite excellent computer resources available to us). Because of the relatively large computer costs, the CCSDT-3(Q_f) calculations were performed only on a subset of 32 geometries required to generate the quadratic force field (harmonic frequencies). The CCSDT-3(Q_f)

TABLE 2: Summary of Anharmonic Vibrational Analyses of *trans*-HNOO[a]

	RHF	MP2	CCSD	CCSD(T)	R-CCSD(T)	CR-CCSD(T)	CCSD(TQ_f)	CCSDT- 3(Q_f)[b]
				EQ				
r(O−O)	1.2876	1.2558	1.2781	1.2951	1.2789	1.2808	1.2901	1.2859
r(N−O)	1.1897	1.3656	1.2677	1.2993	1.2926	1.2880	1.3025	1.3060
r(N−H)	1.0121	1.0299	1.0253	1.0291	1.0272	1.0269	1.0284	1.0286
∠NOO	118.59	116.39	116.97	115.93	116.53	116.54	115.97	115.99
∠HNO	104.69	96.87	100.86	99.76	99.95	100.12	99.63	99.50
ω_1	3609	3378	3417	3367	3393	3396	3375	3374
ω_2	1726	2021	1590	1536	1571	1570	1541	1547
ω_3	1698	1461	1295	1193	1228	1219	1167	1184
ω_4	979	959	1143	1065	1152	1152	1085	1093
ω_5	855	762	696	663	680	681	665	666
ω_6	722	663	842	786	807	811	781	780
Δ_1				−178	−175	−174	−178	−178
Δ_2				−44	−41	−42	−45	−45
Δ_3				−46	−37	−38	−47	−35
Δ_4				−24	−26	−26	−28	−39
Δ_5				−13	−12	−12	−13	−13
Δ_6				−22	−20	−20	−23	−22
ν_1				3189	3218	3221	3197	3196
ν_2				1492	1529	1528	1496	1502
ν_3				1147	1191	1181	1120	1149
ν_4				1042	1126	1126	1057	1054
ν_5				650	668	669	652	652
ν_6				764	788	792	758	757
				NON-STAT				
ω_1	3442	3375	3379	3367	3372	3373	3367	3367
ω_2	1635	1633	1559	1536	1553	1551	1539	1544
ω_3	1147	1393	1145	1193	1168	1156	1170	1169
ω_4	881	1002	1073	1065	1116	1106	1075	1100
ω_5	587	686	667	663	667	666	664	663
ω_6	671	781	811	786	796	797	780	780
Δ_1			−172	−178	−176	−175	−179	−178
Δ_2			−41	−44	−42	−42	−45	−45
Δ_3			−37	−46	−41	−40	−47	−43
Δ_4			−35	−24	−25	−28	−27	−29
Δ_5			−13	−13	−12	−13	−13	−13
Δ_6			−20	−22	−20	−20	−23	−22
ν_1			3206	3189	3196	3198	3188	3188
ν_2			1517	1492	1512	1509	1494	1499
ν_3			1108	1147	1126	1116	1123	1126
ν_4			1038	1042	1091	1078	1047	1071
ν_5			653	650	655	653	650	650
ν_6			791	764	776	777	757	757

[a] Bond distances in Å, angles in deg, harmonic (ω_i) and fundamental (ν_i) frequencies, and total anharmonicities (Δ_i) in cm^{-1}. [b] Quadratic force field combined with CCSD(TQ_f) cubic and quartic force constants.

harmonic frequencies were subsequently corrected with anharmonicities resulting from the CCSD(TQ_f) calculations.

As mentioned earlier, we also used the renormalized and completely renormalized CCSD(T) methods.[12−15] These new methods, which are based on the recently developed formalism of the method of moments of coupled-cluster equations,[12−15,18,22,23] provide improvements in the standard CCSD(T) results when chemical bonds are stretched or broken[12−15,19−21,23−25] and for systems having diradical character.[26] The completely renormalized CCSD(T) approach, [CR−CCSD(T)], is particularly promising in this regard. As mentioned in the Introduction, the diradical character of HNOO has already been acknowledged.[33] We can, thus, expect that the CR−CCSD(T) method provides some improvements in the description of the vibrational spectrum of *trans*-HNOO. Computationally, the R−CCSD(T) and CR−CCSD(T) methods have essentially the same costs as the CCSD(T) approach. They are characterized by the ease of application of the standard CCSD(T) method. Thus, we had no problem performing the R−CCSD(T) and CR−CCSD(T) calculations on the entire grid of 263 geometries, required to generate the quartic force field of HNOO, using the cc-pVTZ basis set. As in all other coupled cluster calculations discussed in this work, we used very tight convergence criteria in the R−CCSD(T) and CR−CCSD(T) calculations (10^{-12} for the maximum change in the SCF density matrix and 10^{-12} for the maximum change in cluster amplitudes).

All R−CCSD(T) and CR−CCSD(T) calculations were performed with the highly efficient system of coupled cluster computer programs[25] which forms part of the electronic structure package GAMESS.[50] We also used GAMESS, along with ACES II, to perform the CCSD(T) calculations on the grid of 263 geometries. The CCSD(TQ_f) and CCSDT-3(Q_f) calculations were performed with the University of Silesia/Michigan State University package of coupled cluster programs which is interfaced with the ACES II Hartree−Fock and integral transformation routines.

The results of anharmonic vibrational analyses of various coupled cluster data available to us are summarized in Table 2. In addition to the aforementioned CCSD(T), R−CCSD(T), CR−CCSD(T), CCSD(TQ_f), and CCSDT-3(Q_f) results, we report the results of the RHF, second-order many-body perturbation theory (MBPT(2) or MP2), and CCSD calculations, which were obtained during the CCSD(T) and post-CCSD(T) calculations. Our discussion focuses on the best results available to us,

obtained with the higher-level CCSD(T), R−CCSD(T), CR−CCSD(T), CCSD(TQ_f), and CCSDT-3(Q_f) methods. The RHF, MP2, and CCSD data are only provided for the completeness of our presentation. It has been well established that the RHF, MP2, and CCSD methods do not provide highly accurate analyses of vibrational spectra. This is particularly true for HNOO, whose electronic structure is similar to that of the complicated ozone molecule, where the effects due to higher-than-doubly excited clusters neglected in the RHF, MP2, and CCSD methods are significant.

We now describe the computational procedures used to determine the quartic force fields of *trans*-HNOO and the corresponding anharmonic vibrational frequencies. As mentioned earlier, all electronic structure results reported in Table 2 were obtained on a common grid of points centered on the CCSD(T) optimum geometry as the reference structure. The high-order numerical differentiations for the HNOO force constants were performed with a new computer code, INTDIF2003,[51] which is capable of computing any force field through sextic order, for any molecule and any number of coordinates, via input information from any order of analytic derivative method, including energy points alone. The code also uses the symmetry of Abelian point groups to minimize the number of displacements. INTDIF2003 contains explicitly programmed central-difference formulas through order 6, does not resort to polynomial fitting schemes, and implements rigorous error control and monitoring. Regardless of the order of the input information, the complete set of force constants in a computed field of maximum order n will be accurate to order $n + 2$. With tight convergence of ab initio wave functions described above, the numerical errors in resulting anharmonic vibrational frequencies can be reduced well below 0.5 cm^{-1}. In our case, the quartic force field of HNOO is determined directly from energy points, and the first numerical contamination in the constants does not appear until order 6. In total, 262 displacements (190 C_s, 72 C_1) were required in addition to the CCSD(T) reference geometry. The step sizes employed for the central-difference computations were 0.01 Å and 0.02 rad for distances and angles, respectively.

In the first set of analyses, labeled EQ in Table 2, the quartic force field at the reference structure was used to interpolate the equilibrium geometry and complete cubic force field at r_e. In these computations, geometric perturbations in the dominant, diagonal stretching, quartic force constants were accounted for by means of approximate quintic constants[52] given by $f_{rrrrr} = (f_{rrrr})^2(f_{rrr})^{-1}$, while the remaining quartic constants were not modulated. In the second set of analyses, labeled NONSTAT, the accurate CCSD(T) reference structure was invoked as a common equilibrium geometry, and the quadratic, cubic, and quartic force constants at this position were used directly in the vibrational analyses for each level of electronic structure theory. The theoretical basis for such a vibrational treatment at a nonstationary geometry is extensively developed by Allen and Császár.[37] The key principle is that at a fixed geometry the error in electronic structure computations usually diminishes greatly as the order of the force constant increases, yet the higher-order force constants are very sensitive to geometric perturbations. Accordingly, in the usual vibrational analysis scheme, substantial errors in the gradients at a given level of theory will cause unnecessary loss of accuracy in corresponding predictions of higher-order force constants merely by giving an insufficiently accurate equilibrium structure. In adopting a better reference geometry, which may be nonstationary at a given level of theory, a first-order shift term is added to the corresponding potential energy surface in order to cancel out spurious nonzero gradients while leaving the more accurate higher-order force constants unchanged. In this sense, the NONSTAT method can be employed to approximate an *equilibrium* vibrational analysis at a higher (or exact) level of theory that is devoid of errors in its r_e structure. The internal coordinates for the NONSTAT vibrational analyses were the OO, NO, and NH bond distances, the valence ∠NOO and ∠HNO bond angles, and the ∠HNOO torsion angle.

We report neither NONSTAT nor EQ anharmonicities in Table 2 for the RHF and MP2 levels of theory because these methods are grossly deficient in their description of the electronic structure of HNOO. In addition, anharmonic corrections via the EQ scheme are omitted for the CCSD vibrational frequencies, because the corresponding optimum geometry is sufficiently removed from the true equilibrium region and the CCSD(T) reference structure as to require an unreliable extrapolation outside our grid points.

After the determination of quartic force fields in the internal coordinate representation, analytic nonlinear transformations to the Cartesian space were performed with the program INTDER-2000,[37,53] which implements **B** tensor formulas[54] through fourth order for all common internal variables. Upon subsequent linear transformations of the force fields to the reduced normal coordinate space, vibrational anharmonic constants (χ_{ij}), vibration−rotation interaction constants (α_i^B), and quartic and sextic centrifugal distortion constants were determined using the formulas of vibrational second-order perturbation theory (VPT2) as applied to the standard vibration−rotation Hamiltonian for semirigid asymmetric top molecules.[55−58] This procedure has been investigated extensively in systematic ab initio studies of vibrational anharmonicity by Allen and co-workers.[34−36,38,52,59] No resonances were excluded from the VPT2 treatment. Although the $2\omega_6$ and ω_3 levels are close-lying in several cases, the anharmonic matrix element between them is too small to anomalously affect the perturbation treatment. Underlying data from the vibrational analysis are presented in the Supporting Information, which includes the quadratic, cubic, and quartic force constants in the internal coordinate space, along with the vibrational anharmonic constants.

Discussion of the Theoretical Results on HNOO

Bond Lengths. All coupled cluster methods predict the OO and NO bond lengths to be within about 0.01 Å. The RHF method predicts the OO bond length to be about 0.1 Å longer than the NO bond length, whereas the MP2 method predicts just the opposite. This illustrates the very well-known inability of the low-order methods to accurately model the electronic structure of many molecular systems, including the isoelectronic ozone molecule.

Harmonic Vibrational Frequencies. Our main interest is in ω_3 and ω_4, the vibrational frequencies corresponding mainly to the NO and OO stretching motions. Just as the bond lengths differ widely for RHF and MP2, so also there is a large difference between these two associated vibrational frequencies, ∼500−700 cm^{-1}. The differences between ω_3 and ω_4 from the CCSD(T), R−CCSD(T), CR−CCSD(T), CCSD(TQ_f), and CCSDT-3(Q_f) methods are 128, 76, 67, 82, and 91 cm^{-1}, respectively, from the EQ results, and 128, 52, 50, 95, and 69 cm^{-1}, respectively, from the NONSTAT results. In brief, our best theoretical methods predict close proximity in NO and OO bond lengths and in the harmonic vibrational frequencies associated with these two bonds.

Fundamental Vibrational Frequencies. Again, our main interest is in ν_3 and ν_4. The difference between ν_3 and ν_4 from

TABLE 3: Comparison of Experimental and Theoretical Vibrational Frequencies, cm^{-1}

frequency	LBSW	LGDS	CCSD(T)	CR−CCSD(T)	CCSD(TQ$_f$)	CCSDT-3(Q$_f$)
ν_1 (NH str)	3287.7	3165.5	3189	3198	3188	3188
ν_2 (HNO bend)	not obs.	1485.5	1492	1509	1494	1499
ν_3 (NO str)	1381.6	1092.3	1147	1116	1123	1126
ν_4 (OO str)	843.2	1054.5	1042	1078	1047	1071
ν_5 (NOO bend)	670.1	not obs.	650	653	650	650
ν_6 (torsion)	790.7	764.0	764	777	757	757

TABLE 4: Isotopic Vibrational Frequency Shifts (cm^{-1}) for *trans*-HNOO

	$\Delta\nu_1$ ($\Delta\omega_1$)	$\Delta\nu_2$ ($\Delta\omega_2$)	$\Delta\nu_3$ ($\Delta\omega_3$)	$\Delta\nu_4$ ($\Delta\omega_4$)	$\Delta\nu_5$ ($\Delta\omega_5$)	$\Delta\nu_6$ ($\Delta\omega_6$)
			DNOO			
CCSD(T)	−794.5 (−905.8)	−261.1 (−273.5)	−5.8[a] (−11.9)	−77.0 (−81.8)	−21.1 (−22.7)	−182.9 (−191.5)
CCSD(TQ$_f$) NONSTAT	−809.5 (−905.8)	−263.1 (−275.0)	−9.5 (−7.6)	−79.5 (−85.4)	−20.9 (−22.6)	−181.2 (−190.1)
LBSW, expt.	−844		−301	−20	−11 (or −82)	−203 (or −132)
			H^{15}NOO			
CCSD(T)	−6.8 (−7.4)	−4.2 (−4.2)	−12.7 (−14.6)	−5.5 (−5.0)	−7.6 (−7.8)	−0.9 (−0.9)
CCSD(TQ$_f$) NONSTAT	−6.8 (−7.4)	−4.2 (−4.3)	−12.6 (−14.3)	−5.3 (−5.1)	−7.6 (−7.8)	−0.8 (−0.9)
			HN^{18}OO			
CCSD(T)	−0.2 (−0.02)	−10.6 (−11.3)	−33.8 (−35.9)	−19.6 (−20.5)	−9.3 (−9.8)	−2.6 (−2.9)
CCSD(TQ$_f$) NONSTAT	−0.2 (−0.01)	−10.5 (−11.3)	−33.0 (−35.2)	−19.7 (−20.6)	−9.3 (−9.8)	−2.6 (−2.9)
LGDS, expt.	0	−10.9	−31.9	−19.7	- -	−2.7
			HNO^{18}O			
CCSD(T)	0.02 (−0.01)	−1.2 (−1.2)	−5.0 (−4.5)	−25.1 (−26.8)	−12.7 (−13.1)	−1.6 (−1.8)
CCSD(TQ$_f$) NONSTAT	0.02 (−0.01)	−1.3 (−1.3)	−4.1 (−4.0)	−25.8 (−27.3)	−12.8 (−13.2)	−1.6 (−1.8)
LGDS, expt.	0	−1.5	−4.3	−25.4	- -	−1.7
			HN^{18}O^{18}O			
CCSD(T)	−0.13 (−0.02)	−11.5 (−12.2)	−38.8 (−40.4)	−46.3 (−48.8)	−21.7 (−22.5)	−4.2 (−4.7)
CCSD(TQ$_f$) NONSTAT	−0.13 (−0.02)	−11.6 (−12.3)	−36.9 (−39.0)	−47.1 (−49.6)	−21.7 (−22.6)	−4.2 (−4.7)
LGDS, expt.	0	−12.1	−36.0	−46.6	- -	−4.4

[a] Excluding $\omega_3 - 2\omega_6$ resonance.

the CCSD(T), R−CCSD(T), CR−CCSD(T), CCSD(TQ$_f$), and CCSDT-3(Q$_f$) methods are 105, 65, 55, 63, and 95 cm^{-1}, respectively, from the EQ results, and 105, 35, 38, 76, and 55 cm^{-1}, respectively, from the NONSTAT results. As expected from the harmonic vibrational frequencies, these fundamentals are predicted to be close together. The anharmonic corrections bring them into even closer proximity than they were predicted at the harmonic level. The agreement between the theoretical $\nu_3 - \nu_4$ differences (particularly those that result from the R−CCSD(T), CR−CCSD(T), and CCSD(TQ$_f$) calculations) and the experimental value of $\nu_3 - \nu_4$ (38 cm^{-1}) is impressive.

Comparison of Theoretical and Experimental Results

To compare the theoretical and experimental results, we combine some essential results from Table 2 with the experimental results of Table 1 into a new Table 3. Our focus above was on the third and fourth bands only. In Table 3, we present all six bands predicted for *trans*-HNOO from our best four theoretical methods and compare them to the experimental results of LBSW and of LGDS.

The results presented in Table 3 strongly favor the assignment of LGDS and disfavor the assignment of LBSW. Consider first the highest frequency band, which is assigned to the NH stretch. The theoretical results, in vacuo, predict this band to occur at ∼3190 cm^{-1} in close proximity to that observed in the Xe matrix by LGDS, 3165.5 cm^{-1}, but far removed from the frequency of 3287 cm^{-1} reported in an Ar matrix by LBSW. Turning to the second band, HNO bend, it was not observed in the assignment of LBSW. LGDS report this band at 1485.5 cm^{-1} to be compared with ∼1500 cm^{-1} from the theoretical results. This is excellent agreement indeed. The third band, NO stretch, is assigned by LGDS at 1092.3 cm^{-1}, in good agreement with the theoretical value of ∼1125 cm^{-1}. However, LBSW assign this band at 1381.6 cm^{-1}, in very poor agreement with theory. The fourth band, OO stretch, is assigned by LGDS at 1054.5 cm^{-1}, in excellent agreement with the theoretical prediction of ∼1060 cm^{-1}. However, LBSW assign the fourth band at 843.2 cm^{-1}, again in very poor agreement with theory. LGDS claim not to have observed the fifth band. LBSW assign this fundamental at 670.1 cm^{-1}, and the computed value is ∼650 cm^{-1}. Finally, the sixth band is reported by LGDS at 764.0 cm^{-1}, in excellent agreement with the theoretical value of ∼765 cm^{-1}. The sixth band reported by LBSW is at 790.7 cm^{-1}.

In summary, there is very good to excellent agreement between the theoretical results and the experimental assignment of LGDS to the HNOO molecule, but very poor agreement with the assignment of LBSW. Further conclusive evidence for the assignment of LGDS is provided by a comparison with the isotopic shift data reported for HNOO by LBSW using deuterium substitution and by LGDS using O-18 substitution.

The theoretical and experimental isotopic shifts are summarized in Table 4. We examine first the deuterium substitution work of LBSW. There was an observed shift of 844 cm^{-1} in the first band and 301 cm^{-1} in the "third" band. (The ν_2 band was assumed undetected.) These shifts are in very poor agreement with the computed shifts of approximately 800 and 10 cm^{-1}, respectively. If we assume that the second observed band is in fact the ν_2 band, then the agreement between theory and experiment is better, ∼260 vs 301 cm^{-1}, although still not acceptable. In any case, there is very poor agreement between theory and LBSW's experiment for both band shifts. The last three bands assigned by LBSW to HNOO also show extremely poor agreement with the computed isotopic shifts, as seen in Table 4. The fourth theoretical band is predicted to exhibit a shift of ∼80 cm^{-1}, whereas the LBSW's experimental assignment places the shift at 20 cm^{-1}. The fifth theoretical band is

predicted to exhibit a shift of ~20 cm^{-1}, whereas the LBSW's experimental assignment places the shift at 11 cm^{-1}. Finally, the sixth theoretical band is predicted to exhibit a shift of ~180 cm^{-1}, whereas the LBSW's experimental assignment places the shift at ~200 cm^{-1}. All in all, there is very poor agreement between the results of our high-level coupled-cluster calculations including anharmonicities and LBSW's experiment for all of the bands.

We turn now to the O-18 isotopic shift work of LGDS. The experimental work reported isotopic shifts for $HN^{18}OO$, $HNO^{18}O$, and $HN^{18}O^{18}O$. Since five bands were observed for each molecule and we have three isotopic variants, there are fifteen bands for which we can compare theory and experiment, Table 4. These fifteen numbers show an astonishing agreement between theory and experiment, usually within 1 cm^{-1}. This very close agreement between theory and experiment provides further evidence for the assignment of LGDS.

Critique of Previous Experimental Results on HNOO, O_3, and HONO

Comparison of Photolytic Precursor. Both the LBSW and LGDS papers utilized the experimental techniques of photolysis, matrix isolation, and infrared spectroscopy. The starting molecule for LBSW was methyl nitrate, CH_3ONO_2, whereas that for LGDS was hydrazoic acid, HN_3, followed by reaction with O_2.

In the work of LGDS, hydrazoic acid is photolyzed to HN and N_2. Generation of the HN precursor from HN_3 has been reported in two other publications.[60,61] So the purported reaction $HN + O_2 \rightarrow HNOO$ is very simple and "clean". Nonetheless, there are numerous bands reported in the matrix isolation experiment that are assigned to "impurity" molecules by LGDS. These include *cis*-HONO, *trans*-HONO, NH_2OH, N_2H_2, H_2O, and CO_2. These impurity molecules could be identified on the basis of other matrix isolation experiments, and upon the behavior of the bands to further annealing and photolysis. Hence, although there were six impurity molecules, the behavior of the various bands due to these molecules was fairly well understood. The assignment of the new bands to HNOO was based upon the simple chemistry of the system and the photolytic behavior of these bands to form both *cis*-HONO and *trans*-HONO molecules in the matrix.

In contrast to the relatively simple system described above, the photolysis of methyl nitrate results in a plethora of bands. LBSW propose that methyl nitrate decomposes via two channels. One channel forms formaldehyde (H_2CO) and hydrogen nitryl (HNO_2), and another forms formaldehyde and HNOO. We count 23 bands in Table 1 of LBSW, due to photoproducts of methyl nitrate after 20 min of photolysis, and 41 bands after 520 min of photolysis. Out of the first 23 bands, five bands were labeled as C, which were eventually assigned to HNOO. A strong factor in the assignment of these bands to HNOO was the excellent agreement between the QCISD[62] (quadratic configuration interaction with singles and doubles) harmonic frequencies for HNOO and the bands labeled as C. The inability of the QCISD theoretical method to accurately model the electronic structure of HNOO will be discussed below.

Comparison to O_3. Given that HNOO is isoelectronic to O_3, it is worthwhile to compare the symmetric and antisymmetric stretching frequencies of ozone to the corresponding bands of HNOO. LGDS stated that "It may be reasonable to think of HNOO as an 'isotopically substituted' ozone molecule, since the NH group is of similar mass to an oxygen atom and is poorly coupled to the lower-frequency modes." The assignment of LGDS of the NO and OO stretching motions is to bands at 1092.3 cm^{-1} and 1054.5 cm^{-1}. These "...frequencies are remarkably close to the ozone stretching frequencies at 1103 cm^{-1} and 1042 cm^{-1} (gas phase)." These two bands are separated by 37.8 cm^{-1} for HNOO and 61 cm^{-1} for O_3. LBSW assigns these two stretching modes at 1382 cm^{-1} and 843 cm^{-1} for HNOO, separated by 539 cm^{-1}, and far removed from the corresponding bands in ozone. In this respect the assignment of LBSW shows substantial similarity to HONO.

Comparison to HONO. Given that HNOO also is isoelectronic with HONO, it is worthwhile to compare the NO and OO stretching frequencies of HNOO with the two NO stretching frequencies of HONO. For purposes of comparison, we will quote our results from LGDS corresponding to the Xe matrix. The results quoted by LBSW in an Ar matrix are very similar.

For *trans*-HONO in a Xe matrix, the NO stretching frequencies occur at 1680 and 794 cm^{-1}; the equivalent modes in *cis*-HONO absorb at 1626 and 842 cm^{-1}. These bands are separated by 886 cm^{-1} and 784 cm^{-1}; this splitting is in reasonable agreement with the 539 cm^{-1} splitting as assigned by LBSW to HNOO. This is completely different from the splitting of the two stretching modes in ozone (~60 cm^{-1}). The NO−OO splitting results of LGDS suggest a molecule with an electronic structure similar to ozone, whereas the results of LBSW suggest an electronic structure closer to HONO than ozone.

On the basis of the coupled cluster results reported above, the electronic structure of HNOO is much more like that of ozone than of HONO. Hence, we expect the vibrational frequencies to be similar to those of ozone and not of HONO, as argued by LGDS and as summarized above. But this bald statement can be further justified by presenting theoretical results on HNOO, HONO, and O_3.

Theoretical Results on Isoelectronic Molecules

HONO. We write three Lewis electron dot structures for HONO below.

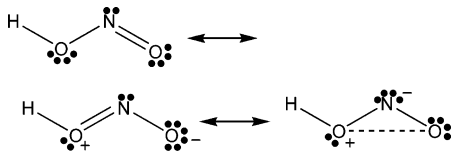

We expect the first structure to dominate; it shows a single bond between the central N and O atoms and a double bond on the terminal pair. The second structure, in which the single and double bonds are interchanged is less important, as there are nonzero formal charges on the two oxygen atoms. The third structure, meant to depict diradical character, also is unimportant for reasons of formal charge. Both the experimental and theoretical work reported in the next paragraph support the assertion that the first resonance structure is dominant.

Table 5 presents experimental and theoretical data related to the NO bond lengths and their associated vibrational frequencies for *trans*-HONO. The experimental difference in the two bond lengths is approximately 0.25 Å; the corresponding computed difference is approximately 0.20 Å at the Hartree−Fock level and 0.24 Å at levels that include correlation [MP4, QCISD, CCSD(T)]. The difference in the frequencies assigned to the N═O and N−O stretching motions is near 900 cm^{-1}, whether by experiment, Hartree−Fock, or one of the more advanced theoretical methods. In particular, the QCISD approach, used by LBSW in their study of HNOO, works reasonably well for HONO. The problem is that the electronic structure of *trans*-

TABLE 5: Experimental and Theoretical Data Associated with the N═O and N−O Stretching Motions of *trans*-HONO[a]

bond length, frequency	expt.,[63,64] gas	HF,[65] 4-31G*	HF, 6-311+G*, this work	MP4,[66] 6-311G**	QCISD, 6-311+G*, LBSW	CCSD(T), 6-311+G*, this work
r(N═O) (Å)	1.170	1.153	1.144	1.175	1.172	1.177
r(N−O) (Å)	1.432	1.345	1.342	1.405	1.415	1.425
ν_2 (N═O)	1700	1820	2032	1767	1781	1736
ν_4 (N−O)	790	970	1079	896	858	827
δ ($\nu_2 - \nu_4$)	910	850	953	871	923	909

[a] The theoretical frequencies are unscaled and harmonic, cm^{-1}. The results from this work were obtained with Gaussian 98.[67]

TABLE 6: Experimental and Computed Harmonic Stretching Frequencies (cm^{-1}) for O_3[a]

method	ω_1 (sym. stretch)	ω_2 (bend)	ω_3 (antisym. stretch)	$\omega_1 - \omega_3$
HF	1537	867	1418	119
MP2	1166	743	2241	−1075
CCSD	1278	762	1267	11
CCSD(T)[30]	1153	716	1054	99
CCSDT[30]	1163	717	1117	46
CCSD(TQ$_f$)[31]	1144	714	1094	50
CCSDT(Q$_f$)[31]	1133	709	1112	21
CISD	1407	816	1535	−128
QCISD	1254	750	996	258
QCISD(T)	1144	707	968	176
expt. (harmonic)	1135	716	1089	46
expt. (fundamental)[68]	1103	701	1042	61

[a] All of the results are with the cc-pVTZ basis set. The QCISD results are from this work, using Gaussian 98.[67] The others are taken from the monograph by Jensen,[69] except as noted.

HNOO has little in common with HONO and a lot in common with ozone, for which QCISD fails (see below). A reasonable performance of QCISD for HONO does not guarantee that the same is true for ozone and HNOO.

O_3. By contrast to the above description of HONO, the electronic structure of ozone is murky indeed. For ozone, *three* Lewis electron dot structures are needed.

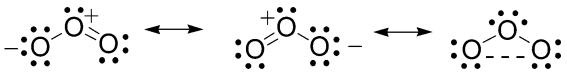

The first two structures show a positive charge on the central atom and are analogous to those for HONO. The last structure has diradical character; it exhibits weakly paired π electrons on the terminal heavy atoms, and zero formal charge on all the atoms. No single resonance structure is predicted to be dominant. From the point of view of theory, the diradical character means that we expect multireference character in the ground state of ozone or the significant role of the connected triply and quadruply excited clusters if we want to retain a single reference description.

It has been known for at least thirty years that a minimum of two electronic configurations is needed to describe the ground state of ozone.[28] In one configuration, two of the four π electrons are in the bonding π molecular orbital, depiction + + +, and two in the nonbonding π molecular orbital, depiction + · −. (The symbols represent the signs of the π lobes from above, and the dot represents a node at that atom.) In another, the two occupied π molecular orbitals are depicted as + + + and + − +.[29] This multireference character has made it difficult to compute vibrational frequencies that are close to the observed frequencies for ozone, see Table 6. A total of 10 theoretical results are presented, and compared to experiment.

The results for the symmetric stretching frequency lie in the range 1133−1278 cm^{-1}, except for those of the HF and CISD methods, which are much higher. All of these results are reasonably close to the harmonic frequency derived from experiment, 1135 cm^{-1}. The bending frequency results all occur in the range 707−762 cm^{-1}, except for those of HF and CISD, which are much higher. This also is in close agreement with (harmonic) experiment, 716 cm^{-1}. The results for the antisymmetric stretch are much worse. The experimental (harmonic) value is 1089 cm^{-1}, and the computed values range from a high of 2241 (MP2) to a low of 968 cm^{-1} [QCISD(T); for a description of the QCISD(T) approach, which is a QCI analogue of CCSD(T), see ref 16]. The range is so large that the MP2 and CISD methods predict the antisymmetric stretching frequency to be *higher* than the symmetric stretching frequency.

Of the results presented in Table 6, the methods[70,71] that show the closest agreement with experiment are CCSD(TQ$_f$) (used in this work) and CCSDT(Q$_f$) [approximated in this work by CCSDT-3(Q$_f$)]. In these two cases, the splitting between the stretching harmonic frequencies is 50 and 21 cm^{-1}, respectively. The CCSD(T) and CCSDT results also are in good agreement with experiment, with splittings of 99 and 46 cm^{-1}, respectively. The QCISD and QCISD(T) results show a splitting between the symmetric and antisymmetric stretching frequencies of 258 and 176 cm^{-1}, respectively, compared to an experimental splitting of 46 cm^{-1}. It is our contention that, just as the QCISD method overestimates the splitting between the symmetric and antisymmetric stretches in ozone, it does the same for the splitting between the NO and OO stretches in imine peroxide. We will substantiate this point with new theoretical results reported in the next subsection.

HNOO. In Table 7 we gather the bond lengths and frequencies primarily associated with the NO and OO stretching motions for *trans*-HNOO. Included are the QCISD results from LBSW, and new results that we have obtained using the QCISD(T) theoretical method. The QCISD and QCISD(T) data are compared to a selection of our best coupled-cluster results, obtained with the CR−CCSD(T), CCSD(TQ$_f$), and CCSDT-3(Q$_f$) methods.

The results in Table 7 show that Hartree−Fock theory is incapable of describing the competition between the NO and OO bonds for electron density, as we have discussed previously. The second column shows the QCISD result from LBSW. Compared to the Hartree−Fock result, the QCISD method predicts a lengthening of both the NO bond (0.07 Å) and the OO bond (0.04 Å); the NO distance is still 0.07 Å *shorter* than the OO bond. This has substantial implications for the corresponding frequencies. The NO stretch is predicted at 1391 cm^{-1} and the OO stretch at 841 cm^{-1}, for a separation of 550 cm^{-1}, when the QCISD method is employed. This is not as large as the 719 cm^{-1} separation predicted by the Hartree−Fock method, but it is substantially greater than the values predicted by our best coupled cluster results, as shown in Tables 2, 3, and 7. The QCI formalism is unable to produce the very small, ca. 50 cm^{-1} difference between ν_3 and ν_4 observed in our calculations and experiment, since even the better QCISD(T) approach produces a difference of ∼200 cm^{-1} between these two frequencies.

TABLE 7: Pertinent Theoretical Data Associated with the NO and OO Stretching Motions of *trans*-HNOO[a]

bond length, frequency	HF, this work	LBSW, QCISD	QCISD(T) this work	CR−CCSD(T) this work[b]	CCSD(TQ$_f$) this work[b]	CCSDT-3(Q$_f$) this work[b]
r(NO) (Å)	1.190	1.263	1.298	1.288	1.303	1.306
r(OO) (Å)	1.288	1.329	1.305	1.281	1.290	1.286
ω_3 (NO str)	1698	1391	1152	1219 (1156)	1167 (1170)	1184 (1169)
ω_4 (OO str)	979	841	948	1152 (1106)	1085 (1075)	1093 (1100)
δ ($\omega_3 - \omega_4$)	719	550	204	67 (50)	82 (95)	91 (69)

[a] The QCISD and QCISD(T) results employ the 6-311+G* basis set. The QCISD(T) values were obtained with Gaussian 98.[67] [b] For purposes of comparing frequencies, ω_3 and ω_4 EQ values are given with corresponding NONSTAT results in parentheses.

Our best theoretical calculations, including the calculations performed with the state-of-the-art CR−CCSD(T), CCSD(TQ$_f$), and CCSDT-3(Q$_f$) methods, predict the NO and OO bond lengths to be practically identical. In consequence, the corresponding vibrational frequencies are predicted to be much closer together. Clearly, our best theoretical methods reproduce the observed ca. 38 cm^{-1} difference between ν_3 and ν_4 extremely well. The QCISD and QCISD(T) methods cannot do it.

The three Lewis electron dot structures for HNOO are analogous to those for ozone.

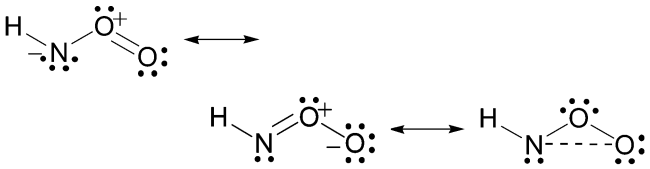

Our theoretical structure and frequency results for HNOO predict it to be similar to that of ozone, and not similar to HONO. This fits with simple predictions based upon Lewis electron dot structures.

In summary, these results on HONO, O_3, and HNOO show that the RHF and QCISD methods cannot adequately describe the electronic structure of the latter two molecules. This forces us to question the assignment reported by LBSW, who used the QCISD methodology to support their findings. By contrast, the more advanced of the coupled cluster results on ozone, employing methods used in this work, are excellent, and so we expect that they also describe the essential features of HNOO.

Conclusions

The *trans*-HNOO molecule has OO and NO bond lengths and vibrational stretching frequencies close together from theory and experiment. According to the results of LGDS, the stretching frequencies appear at 1092 and 1055 cm^{-1} in a Xe matrix. Computed stretching frequencies using advanced coupled cluster methodologies, particularly CR−CCSD(T), CCSD(TQ$_f$), and CCSDT-3(Q$_f$), corrected for anharmonicities, are in excellent agreement with this result for the trans isomer.

We believe that the experimental results of LBSW do not provide strong evidence for the formation of HNOO from photolysis of CH_3ONO. There are too many photoproducts in the matrix and the reaction is too complex to identify HNOO as a primary product. Furthermore, the QCISD theoretical method, used by LBSW to argue in favor of their assignment of the observed spectrum, is not to be trusted for the HNOO molecule as indicated by results in Table 7; the QCISD approach and its QCISD(T) extension to account for the effect of triples do not provide good results for the isoelectronic ozone, Table 6.

Contrary to the poor results obtained from QCISD and QCISD(T), we believe that the results provided by the CCSD(T) approach and the more advanced coupled cluster methods used in this work are trustworthy on the basis of their ability to provide *very good* results for ozone. The CCSD(T) method utilizing a basis set such as cc-pVTZ has been shown to provide high-quality results for a wide range of molecules.[72] Nonetheless, we do recognize that *excellent* theoretical vibrational frequencies for molecules such as ozone may require a higher level of theory than CCSD(T). Hence, we have included in our study the results of some of these more advanced methods accounting, in particular, for the combined effect of triply and quadruply excited clusters. Kucharski and Bartlett[31] have shown that connected quadruple excitations are needed for quantitative structure and frequency predictions of ozone.

In the work reported here we must decide whether the NO and OO stretching frequencies occur at 1382 and 843 cm^{-1} as reported by LBSW, or at 1092 and 1055 cm^{-1} as reported by LGDS. For such a large difference, the CCSD(T) method with the cc-pVTZ basis set seems more than adequate, although we decided to be very critical and tested the reliability of the CCSD(T) approach in the calculations for HNOO by performing a large number of additional calculations with the R−CCSD(T), CR−CCSD(T), CCSD(TQ$_f$), and CCSDT-3(Q$_f$) approaches. Our studies indicate that the CCSD(T) results are improved upon by the R−CCSD(T), CR−CCSD(T), CCSD(TQ$_f$), and CCSDT-3(Q$_f$) methods, although CCSD(T) is capable of providing a reasonable description of the HNOO geometry and spectrum. Our excellent agreement between the experimental and theoretical CCSD(TQ$_f$) and CCSDT-3(Q$_f$) vibrational frequencies of HNOO is in accord with the similar agreement observed by Kucharski and Bartlett for ozone.[31] It is very interesting to observe that the recently proposed CR−CCSD(T) method of Kowalski and Piecuch,[12,13] which is not much more expensive than CCSD(T), provides an excellent description of the vibrational spectrum of *trans*-HNOO. The CR−CCSD(T) results are better than those obtained with the standard CCSD(T) approximation when the NO and OO stretches are considered. This is probably related to a partially multireference or diradical character of HNOO, which should be well described by the CR−CCSD(T) approach.

Acknowledgment. This work was partially supported by the National Center for Supercomputing Applications under grant number CHE990012N and utilized the Exempler X-Class machine billie.ncsa.uiuc.edu at the National Center for Supercomputing Applications, University of Illinois at Urbana-Champaign. The majority of the coupled cluster calculations were performed on a 32-processor Origin 3400 system at Michigan State University obtained through a grant from the National Science Foundation, Chemical Instrumentation #9974834. Some of our work was performed on a Beowulf cluster at Calvin College, obtained through a grant from the National Science Foundation, NSF-MRI Grant 0079739. The Dreyfus Foundation provided financial support to A.R.B. and S.A.S. through a Camille and Henry Dreyfus Scholar/Fellow Program for Undergraduate Institutions grant to RDK. The latter acknowledges

Calvin College for a Calvin Research Fellowship and a sabbatical leave that supported this work. Acknowledgment is made to the Donors of the American Chemical Society Petroleum Research Fund, for partial support of this research through the Undergraduate Faculty Sabbatical program. The work at the University of Georgia was supported by the U.S. Department of Energy, Office of Basic Energy Sciences, Combustion Program (Grant DE-FG02-97ER14748) and SciDAC Computational Chemistry Program (Grant DE-FG02-01ER15226). The work at Michigan State University was supported by the Department of Energy, Office of Basic Energy Sciences, SciDAC Computational Chemistry Program (Grant DE-FG02-01ER15228) and by the Alfred P. Sloan Foundation (awards provided to P.P.).

Appendix

We mention pertinent data related to the cis and trans isomers of HNOO. In our previous paper, ref 2, we presented CCSD(T) harmonic vibrational frequencies for both the cis and the trans isomers. The six frequencies for the cis are 3268, 1502, 1215, 1062, 656, and 874 cm^{-1}. The corresponding values for the trans are 3379, 1553, 1193, 1068, 670, and 770 cm^{-1}. (These harmonic values are very close to those reported in this work, using a different basis set.) In each case, the first vibrational frequency corresponds mainly to the NH stretch, and the last to the torsional motion.

The main differences between the two molecules are in the first and the last frequency, as we would expect from qualitative arguments about the two molecules. For example, in the cis molecule there can be intramolecular hydrogen bonding, leading to a lower NH stretching frequency, exactly as we observe computationally. The NH stretching frequency for the cis isomer is about 100 cm^{-1} *lower* than that of the trans. Conversely, such intramolecular interaction should cause the torsional frequency to be *higher* for the cis as compared to the trans isomer. Again, this is exactly what we observe computationally, and by about 100 cm^{-1}.

Now, our unpublished work shows that the anharmonic corrections are about the same for both the cis and the trans isomers. This correction is about -175 cm^{-1} for the NH stretch, and -20 cm^{-1} for the torsional motion. Therefore, our expected theoretical placement of the NH stretch for the cis isomer is $3268 - 175 = 3093$ cm^{-1}. But LGDS report their first band at 3165.5 cm^{-1}, for a difference of 73 cm^{-1}. Likewise, the expected theoretical placement of the torsional frequency is $874 - 20 = 854$ cm^{-1}. But LGDS report the lowest frequency band at 764 cm^{-1}, for a difference of 90 cm^{-1}. The comparison between theory and experiment is even worse if we use the experimental data of LBSW.

Looking now at the close agreement between theory (trans) and experiment for all observed bands presented in Table 3, we see that such differences as 73 and 90 cm^{-1} are untenable. It is mainly for this reason that we reject the assignment of the experimental bands to the cis isomer.

Supporting Information Available: Additional tables of theoretical results on *trans*-HNOO. These tables include quadratic, cubic, and quartic force constants, as well as anharmonic constants. This material is available free of charge via the Internet at http://pubs.acs.org.

References and Notes

(1) Ling, P.; Boldyrev, A. I.; Simons, J.; Wight, C. A. *J. Am. Chem. Soc.* **1998**, *120*, 12327−12333.
(2) Laursen, S. L.; Grace, J. E., Jr.; DeKock, R. L.; Spronk, S. A. *J. Am. Chem. Soc.* **1998**, *120*, 12583−12594.
(3) Jacox, M. E. *Chem. Soc. Rev.* **2002**, 108−115.
(4) Badger, R. M. *J. Chem. Phys.* **1934**, *2*, 128−131.
(5) Badger, R. M. *J. Chem. Phys.* **1935**, *3*, 710−714.
(6) Cioslowski, J.; Liu, G.; Castro, R. A. M. *Chem. Phys. Lett.* **2000**, *331*, 497−501.
(7) Čížek, J. *J. Chem. Phys.* **1966**, *45*, 4256−4266.
(8) Čížek, J. *Adv. Chem. Phys.* **1969**, *14*, 35−89.
(9) Bartlett, R. J. In *Modern Electronic Structure Theory, Part I*; Yarkony, D. R., Ed.; World Scientific: Singapore, 1995; pp 1047−1131.
(10) Crawford, T. D.; Schaefer, H. F., III. *Rev. Comput. Chem.* **2000**, *14*, 33−136.
(11) Paldus, J.; Li, X. *Adv. Chem. Phys.* **1999**, *110*, 1−175.
(12) Piecuch, P.; Kowalski, K. In *Computational Chemistry: Reviews of Current Trends*; Leszczynski, J., Ed.; World Scientific: Singapore, 2000; Vol. 5, pp 1−104.
(13) Kowalski, K.; Piecuch, P. *J. Chem. Phys.* **2000**, *113*, 18−35.
(14) Piecuch, P.; Kowalski, K.; Pimienta, I. S. O.; McGuire, M. J. *Int. Rev. Phys. Chem.* **2002**, *21*, 527−655.
(15) Piecuch, P.; Kowalski, K.; Fan, P.-D.; Pimienta, I. S. O. In *Advanced Topics in Theoretical Chemical Physics*, Vol. 12 of *Progress in Theoretical Chemistry and Physics*; Maruani, J., Lefebvre, R., Brandas, E., Eds.; Kluwer: Dordrecht, 2003; pp 119−206.
(16) Raghavachari, K.; Trucks, G. W.; Pople, J. A.; Head-Gordon, M. *Chem. Phys. Lett.* **1989**, *157*, 479−483.
(17) Kucharski, S. A.; Bartlett, R. J. *J. Chem. Phys.* **1998**, *108*, 9221−9226.
(18) Kowalski, K.; Piecuch, P. *J. Chem. Phys.* **2000**, *113*, 5644−5652.
(19) Kowalski, K.; Piecuch, P. *Chem. Phys. Lett.* **2001**, *344*, 165−175.
(20) Piecuch, P.; Kucharski, S. A.; Kowalski, K. *Chem. Phys. Lett.* **2001**, *344*, 176−184.
(21) Piecuch, P.; Kucharski, S. A.; Spirko, V.; Kowalski, K. *J. Chem. Phys.* **2001**, *115*, 5796−5804.
(22) Piecuch, P.; Kowalski, K.; Pimienta, I. S. O.; Kucharski, S. A. In *Low-Lying Potential Energy Surfaces*; Hoffmann, M. R., Dyall, K. G., Eds.; American Chemical Society: Washington, DC, 2002; Vol. 828, pp 31−64.
(23) Piecuch, P.; Kowalski, K.; Pimienta, I. S. O. *Int. J. Mol. Sci.* **2002**, *3*, 475−497.
(24) McGuire, M. J.; Kowalski, K.; Piecuch, P. *J. Chem. Phys.* **2002**, *117*, 3617−3624.
(25) Piecuch, P.; Kucharski, S. A.; Kowalski, K.; Musiał, M. *Comput. Phys. Commun.* **2002**, *149*, 71−96.
(26) Özkan, I.; Kinal, A.; Balci, M. *J. Phys. Chem. A* **2004**, *108*, 507−514.
(27) Finlayson-Pitts, B. J.; Pitts, J. N. *Chemistry of the Upper and Lower Atmosphere: Theory, Experiments, and Applications*; Academic Press: New York, 1999.
(28) Hay, P. J.; Goddard, W. A., III. *Chem. Phys. Lett.* **1972**, *14*, 46−48.
(29) Yamaguchi, Y.; Frisch, M. J.; Lee, T. J.; Schaefer, H. F., III; Binkley, J. S. *Theor. Chim. Acta* **1986**, *69*, 337−352.
(30) Watts, J. D.; Bartlett, R. J. *J. Chem. Phys.* **1998**, *108*, 2511−2514.
(31) Kucharski, S. A.; Bartlett, R. J. *J. Chem. Phys.* **1999**, *110*, 8233−8235.
(32) Lee, T. J.; Scuseria, G. E. *J. Chem. Phys.* **1990**, *93*, 489−494.
(33) Fueno, T.; Yokoyama, K.; Takane, S.-y. *Theor. Chim. Acta* **1992**, *82*, 299−308.
(34) Clabo, D. A., Jr.; Allen, W. D.; Remington, R. B.; Yamaguchi, Y.; Schaefer, H. F., III. *Chem. Phys.* **1988**, *123*, 187−239.
(35) Allen, W. D.; Yamaguchi, Y.; Császár, A. G.; Clabo, D. A., Jr.; Remington, R. B.; Schaefer, H. F., III. *Chem. Phys.* **1990**, *145*, 427−466.
(36) Thiel, W.; Scuseria, G. E.; Schaefer, H. F., III; Allen, W. D. *J. Chem. Phys.* **1988**, *89*, 4965−4975.
(37) Allen, W. D.; Császár, A. G. *J. Chem. Phys.* **1993**, *98*, 2983−3015.
(38) East, A. L. L.; Johnson, C. S.; Allen, W. D. *J. Chem. Phys.* **1993**, *98*, 1299−1328.
(39) Dunning, T. H., Jr. *J. Chem. Phys.* **1989**, *90*, 1007−1023.
(40) Stanton, J. F.; Gauss, J.; Watts, J. D.; Nooijen, M.; Oliphant, N.; Perera, S. A.; Szalay, P. G.; Lauderdale, W. J.; Kucharski, S. A.; Gwaltney, S. R.; Beck, S.; Balkova, A.; Bernholdt, D. E.; Baeck, K. K.; Rozyczko, P.; Sekino, H.; Hober, C.; Bartlett, R. J. ACES II; Quantum Theory Project: University of Florida.
(41) Salter, E. A.; Trucks, G. W.; Bartlett, R. J. *J. Chem. Phys.* **1989**, *90*, 1752−1766.
(42) Salter, E. A.; Bartlett, R. J. *J. Chem. Phys.* **1989**, *90*, 1767−1773.
(43) Oliphant, N.; Adamowicz, L. *J. Chem. Phys.* **1991**, *95*, 6645−6651.
(44) Kucharski, S. A.; Bartlett, R. J. *Theor. Chim. Acta* **1991**, *80*, 387−405.
(45) Kucharski, S. A.; Bartlett, R. J. *J. Chem. Phys.* **1992**, *97*, 4282−4288.
(46) Piecuch, P.; Adamowicz, L. *J. Chem. Phys.* **1994**, *100*, 5792−5809.

(47) Noga, J.; Bartlett, R. J.; Urban, M. *Chem. Phys. Lett.* **1987**, *134*, 126−132.
(48) Noga, J.; Bartlett, R. J. *J. Chem. Phys.* **1987**, *86*, 7041−7050. Erratum, **1988**, *89*, 3401.
(49) Scuseria, G. E.; Schaefer, H. F., III. *Chem. Phys. Lett.* **1988**, *152*, 382−386.
(50) Schmidt, M. W.; Baldridge, K. K.; Boatz, J. A.; Elbert, S. T.; Gordon, M. S.; Jensen, J. H.; Koeski, S.; Matsunaga, N.; Nguyen, K. A.; Su, S. J.; Windus, T. L.; Dupuis, M.; Montgomery, J. A., Jr. *J. Comput. Chem.* **1993**, *14*, 1347−1363.
(51) Allen, W. D.; INTDIF2003 is an abstract program written by Wesley D. Allen for *Mathematica* (Wolfram Research, Inc., Champaign, Illinois) to perform general numerical differentiations to high orders of electronic structure data, 2003.
(52) East, A. L. L.; Allen, W. D.; Klippenstein, S. J. *J. Chem. Phys.* **1995**, *102*, 8506−8532.
(53) Allen, W. D.; INTDER2000 is a general program developed by Wesley D. Allen and co-workers which performs various vibrational analyses and higher-order nonlinear transformations among force field representations, 2000.
(54) Allen, W. D.; Császár, A. G.; Szalay, V.; Mills, I. M. *Mol. Phys.* **1996**, *89*, 1213−1221.
(55) Nielsen, H. H. *Rev. Mod. Phys.* **1951**, *23*, 90−136.
(56) Mills, I. M. In *Molecular Spectroscopy: Modern Research*; Rao, K. N., Mathews, C. W., Eds.; Academic Press: New York, 1972; Vol. 1, pp 115−140.
(57) Papousek, D.; Aliev, M. R. *Molecular Vibrational−Rotational Spectra*; Elsevier: Amsterdam, 1982.
(58) Watson, J. K. G. In *Vibrational Spectra and Structure*; Durig, J. R., Ed.; Elsevier: Amsterdam, 1977; Vol. 6, pp 1−89.
(59) Aarset, K.; Császár, A. G.; Sibert, E. L., III; Allen, W. D.; Schaefer, H. F., III; Klopper, W.; Noga, J. *J. Chem. Phys.* **2000**, *112*, 4053−4063.
(60) Laursen, S. L.; Delia, A. E.; Mitchell, K. *J. Phys. Chem. A* **2000**, *104*, 3681−3692.
(61) Himmel, H.-J.; Junker, M.; Schnöckel, H. *J. Chem. Phys.* **2002**, *117*, 3321−3326.
(62) Pople, J. A.; Head-Gordon, M.; Raghavachari, K. *J. Chem. Phys.* **1987**, *87*, 5968−5975.
(63) Finnigan, D. J.; Cox, A. P.; Brittain, A. H.; Smith, J. G. *J. Chem. Soc., Faraday Trans. 2* **1972**, *68*, 548−565.
(64) Deeley, C. M.; Mills, I. M. *Mol. Phys.* **1985**, *54*, 23−32.
(65) Nakamura, S.; Takahashi, M.; Okazaki, R.; Morokuma, K. *J. Am. Chem. Soc.* **1987**, *109*, 4142−4148.
(66) Coffin, J. M.; Pulay, P. *J. Phys. Chem.* **1991**, *95*, 118−122.
(67) Frisch, M. J.; Trucks, G. W.; Schlegel, H. B.; Scuseria, G. E.; Robb, M. A.; Cheeseman, J. R.; Zakrzewski, V. G.; Montgomery, J. A., Jr.; Stratmann, R. E.; Burant, J. C.; Dapprich, S.; Millam, J. M.; Daniels, A. D.; Kudin, K. N.; Strain, M. C.; Farkas, O.; Tomasi, J.; Barone, V.; Cossi, M.; Cammi, R.; Mennucci, B.; Pomelli, C.; Adamo, C.; Clifford, S.; Ochterski, J.; Petersson, G. A.; Ayala, P. Y.; Cui, Q.; Morokuma, K.; Malick, D. K.; Rabuck, A. D.; Raghavachari, K.; Foresman, J. B.; Cioslowski, J.; Ortiz, J. V.; Stefanov, B. B.; Liu, G.; Liashenko, A.; Piskorz, P.; Komaromi, I.; Gomperts, R.; Martin, R. L.; Fox, D. J.; Keith, T.; Al-Laham, M. A.; Peng, C. Y.; Nanayakkara, A.; Gonzalez, C.; Challacombe, M.; Gill, P. M. W.; Johnson, B.; Chen, W.; Wong, M. W.; Andres, J. L.; Gonzalez, C.; Head-Gordon, M.; Replogle, E. S.; Pople, J. A. *Gaussian 98*, revision A.5; Gaussian, Inc.: Pittsburgh, PA, 1998.
(68) Schriver-Mazzuoli, L.; Schriver, A.; Lugez, C.; Perrin, A. *J. Mol. Spectrosc.* **1996**, *176*, 85−94.
(69) Jensen, F. *Introduction to Computational Chemistry*; John Wiley & Sons: New York, 1999.
(70) All of the theoretical methods quoted in Table 6 choose a single determinant as their reference state. The highest level work reported to date on ozone is a multireference study described as icMRCI+Q/cc-pVQZ using a CASSCF(12,9) reference space. This method was used to generate a grid for the global potential energy surface. The theoretical values are within one or two wavenumbers of the experimental result. See the following reference.
(71) Siebert, R.; Fleurat-Lessard, P.; Schinke, R.; Bittererová, M.; Farantos, S. C. *J. Chem. Phys.* **2002**, *116*, 9749−9767.
(72) Helgaker, T.; Gauss, J.; Jørgenson, P.; Olsen, J. *J. Chem. Phys.* **1997**, *106*, 6430−6440.